Full Paper

EFFECTS OF TITANIA ADDITIVE ON PHASES DEVELOPMENT AND HARDNESS OF SPARK PLASMA SINTERED MULLITE-CARBON-MnO_2 CERAMIC COMPOSITE

F. O. Aramide
Department of Metallurgical and Materials Engineering, Federal University of Technology, Akure, Nigeria.
foaramide@futa.edu.ng

A. P. I. Popoola
Department of Chemical, Metallurgical and Materials Engineering, Tshwane University of Technology, Staatsartillerie Road, Pretoria West, South Africa.

ABSTRACT

Effects of varied contents of titania on the phase development and properties of spark plasma sintered (SPS) mullite-carbon-MnO_2 ceramic composite was investigated. The raw materials used were kaolin clay, graphite, manganese oxide and titania. Samples were prepared by blending pre-calculated amounts of raw materials in Turbular mixer at a speed of 72 rev/min. The homogenous mixture were sintered in the SPS machine at 1000°C at a sintering pressure of 40 MPa, heating rate of 50°C/min and holding time of 10 min in a graphite die of 20mm. The phases in the sintered samples were characterized using x-ray diffractometry analysis (XRD). Microstructure of the samples were examined using scanning electron microscope (SEM). Harness of the sintered samples was also investigated using Vickers hardness tester. It was observed that the phases evolved in the sample were influenced by titania content. The presence of $Mn2O_3$ in the sample lead to formation of silimanite in preference to mullite when sintered 1000°C. 12% titania in sample D aided development of mullite phases within the sample. Presence of 16% titania and $Mn2O_3$ led to development of carbides like Al_4C_3 and $Al_4Si_2C_5$ in sample E. Addition of titania to the samples progressively improved on densification of the samples with increased titania contents. It was concluded that the development of carbides within the ceramic matrix is responsible for the increased hardness of the sample.

Keywords: phase developments; hardness; sintering; carbon based ceramic composite; mullite.

1. INTRODUCTION

Mullite has been reported to be a promising candidate for high temperature application. This is due to its high refractoriness, low thermal expansion, creep rate and thermal conductivity. It also has good chemical and thermal stability with high thermal shock resistance (Aksay et al. 1991; Sacks et al. 1990; Kaya et al. 2002). Developing this mullite fibre within a ceramic matrix as reinforcing phase will tremendously improve on the mechanical properties of such material.

It has been reported that monolithic ceramics applications have been limited due to their intrinsic brittleness which make them unreliable in many applications (Aramide and Popoola, 2017; Naskar et al. 2004; Tressler, 1999). To mitigate this problem, many researchers have device means for strengthening the ceramic to improve on their fracture toughness. This is usually achieved through three different methods as reported by various researchers. Namely by incorporating reinforcing phases (either as fibres or particulate) within the ceramic matrix (Callister, 2007; Dag and Annette, 2007; Low et al. 1994; Li et al, 2012a; Li et 2012b; Yang et al. 2012a; Kaya et al. 2002; Yang et al. 2012b; Stoll et al. 2006; Ye et al. 2008). Another method is by engineering spherical pores within the material which arrest crack propagation as soon as it is formed (Guo et al. 2012; Jang et al. 2008; Gong et al. 2005; Kanaun and Tkachenko, 2008). The third method is phase-transformation toughening as in the case of partially and fully stabilized zirconia ceramics (Osendi and Baudin, 1996; Moya and Osendi, 1983; Aramide et al. 2015). The main aim of this work is to investigate the effects of titania additive on the phases development and hardness of the spark plasma sintered mullite-carbon-MnO_2 ceramic composite.

2. MATERIALS AND METHODS

2.1. Sample Preparation:

Commercially available titanium dioxide (titania) and manganese dioxide powders (purity, 98%; 2-5 µm; Hubei Duobo New Ceramic Materials Co., Ltd.,Wuhan, China), graphite powder (purity, 99.5%; < 50 µm; Merck KGaA, 64271 Darmstadt, Germany) and kaolinite from kaolin clay sourced from Okpella deposit, Edo State, Nigeria (98.98 % kaolinite) were used as the raw materials.

The pre-calculated amount of each of the raw materials were mixed together in a Turbula mixer at 72 Rev/min for 8 hours. A pre-determined amount of the homogenous mixture were poured in a graphite die of 20 mm internal diameter and sintered in a spark plasma sintering machine at 1000°C at a sintering pressure of 40 MPa, heating rate of 50°C/min and holding time of 10 min. Table 1 shows the composition of the samples based on the raw materials used.

2.2. Characterization:

The sintered samples were shot blasted to clean the surfaces. The samples' densities were then measured using Archimedes' principle. These densities were compared with the

theoretical/calculated densities of the samples to arrive at the various sample percentage densification.

The sintered sample was prepared for XRD analysis using a back loading preparation method. It was analysed with a Malvern Panalytical AERIS diffractometer with PIXcel detector and fixed slits with Fe filtered Co-K α radiation the scanning angle from 2 θ = 10° to 2 θ = 90°, and a scanning rate of 4° /min. The phases were identified using X' Pert Highscore plus software.

Table 1. Showing the different sample composition

Designation	Kaolin (wt %)	Graphite (wt %)	Manganese dioxide (wt %)	Titania (wt %)
Sample A	75	20	5	0
Sample B	71	20	5	4
Sample C	67	20	5	8
Sample D	63	20	5	12
Sample E	59	20	5	16

2.3. Vickers hardness:

The hardness tests were carried out using a Vickers hardness tester (Wolpert-430SV, Wolpert Wilson Instruments, Aachen, Germany) under a load of 5 kg for 15 s.

3. RESULTS AND DISCUSSION

Figure 1 shows the xrd patterns of the various sintered sample with the identified phases while Table 2, Figure 2 shows the scanning electron microscope (SEM) images of the various sintered samples while Figures 3, 4 and 5 show the effect of titania contents on the percentage densification, porosity and hardness respectively.

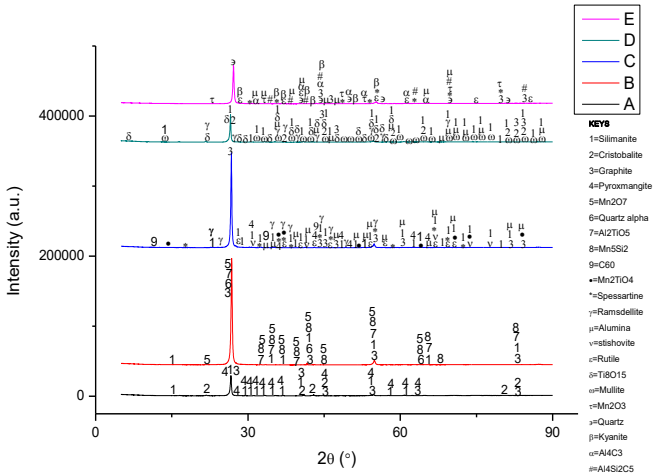

Figure 1. xrd patterns of various sample showing the identified phases

Table 2. Showing the densification, porosity and Vickers hardness of the various sample

Designation	Densification (%)	Porosity (%)	Vickers hardness (Hv)
Sample A	89.17	10.83	455
Sample B	92.33	7.67	499
Sample C	95.46	4.54	564
Sample D	97.86	2.14	644
Sample E	99.11	0.89	817

3.1. Effect of titania contents on the phases developed in the sintered samples:

Figure 1 shows the different phases identified in various sintered sample, Figure 2 also shows the scanning electron micrographs of the various sintered sample. From the Figure 1 it is observed that for sample A (0% titania), the identified phases are silimanite, cristobalite, graphite and pyroxmangite (depicted in Figure 2). From Table 1, it is observed that the raw materials from which the sample was made are kaolinite (from kaolin) graphite and manganese dioxide (Mn_2O_3). The formation of silimanite could be linked to the dehydroxilation of the kaolinite content when it was subjected to heating. The dehydroxilation of kaolinite takes place around 400-650°C through the following reaction (Aramide 2012; Lamberov et al. 2012; Varga, 2007):

$$Al_2O_5.2SiO_2.2H_2O \rightarrow Al_2O_3.2SiO_2 + 2H_2O\ (g)$$
Kaolinite → Metakaolin.

But in the presence of Mn_2O_3, the metakaolin decomposed to silimanite and silica via the chemical reaction:

$$Al_2O_3.2SiO_2 \rightarrow Al_2O_3.SiO_2 + SiO_2$$
Metakaolin → Silimanite + Silica

The silica then reacts with the Mn_2O_3, to form pyroxmangite (a manganese silicate) via the chemical equation:

$$2SiO_2 + Mn_2O_3 \rightarrow 2MnSiO_3 + \frac{1}{2}O_2\ (g)$$
Silica → Pyroxmangite

The cristobalite (an allotrope of silica) could be excess silica from the decomposition of metakaolin. It is inferred that the presence of Mn_2O_3 in the sample lead to formation of silimanite in preference to mullite when sintered at 1000°C.

Moreover, when 4% titania was added to the sample (sample B) the phases identified in it are silimanite, graphite, Mn_2O_7, quartz (another allotrope of silica), Al_2TiO_4 and Mn_5Si_2. It observed that the presence of titania prevented the formation of pyroxmangite, instead an oxygen-rich manganese oxide (Mn_2O_7), manganese silicide, and aluminium titanate (Al_2TiO_4) were formed.

Furthermore, with the addition of 8% titania (sample C) the identified phases are silimanite, carbon 60 (C60), Mn_2TiO_4, spessartine ($Mn_3Al_2Si_3O_{12}$), ramsdellite (MnO_2), graphite, alumina, rutile, stishovite (a form of silica) and pyroxmangite. Moreover, when 12% titania was added to the sample (sample D) the phases identified in it are silimanite, graphite, cristobalite, ramsdellite, alumina, Ti_8O_{15} and mullite. It can be inferred that 12% titania in the sample aided the formation of mullite phases within the sample. However, with the addition of 16% titania in the sample (sample E), the identified phases are kyanite (an allotrope of silimanite), spessartine, alumina, rutile, Mn_2O_3, quartz, Al_4C_3 and $Al_4Si_2C_5$. It can be inferred that the presence of 16% titania and Mn_2O_3 led to the formation of carbides like Al_4C_3 and $Al_4Si_2C_5$ in the sample.

3.2. Effect of titania contents on densification, porosity and hardness of the sintered samples:

3.2.1. Densification

Figure 3 shows the effect of titania contents on the percentage densification of the sintered samples. From the figure it is observed that the percentage densification of the samples increased with the titania contents. It is observed that the percentage densification of sample with 0% titania (sample A) was 89.17%. However, when the titania content was increased to 4% (sample B), its densification increased to 92.33%. At 8% titania content (sample C) the densification of the sample is observed to further increased to 95.46%. Moreover, at 12% titania content (sample D) the densification of the sample is observed to increase to 97.86%. The densification of the sample reached its maximum of 99.11% when the titania content was increased to 16%. This agrees with the findings Aramide et al. (2017) who reported that addition of titania

improved on the densification of the samples they reported on. Titania can act as sintering aid in ceramic.

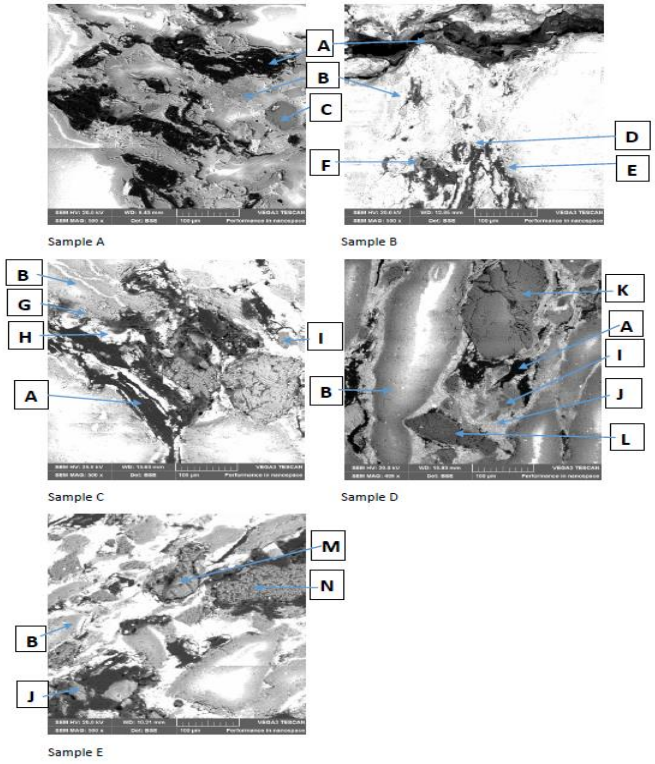

Figure 2 Showing the scanning electron micrograph of the various samples: A=graphite; B=silimanite; C=pyroxmangite; D= Al_2TiO_4; E= Mn_5Si_2; F= Mn_2O_7; G= Mn_2TiO_4; H= spessartine; I= ramsdellite; J=, alumina; K= Ti_8O_{15}; L= mullite; M= Al_4C_3 and N= $Al_4Si_2C_5$.

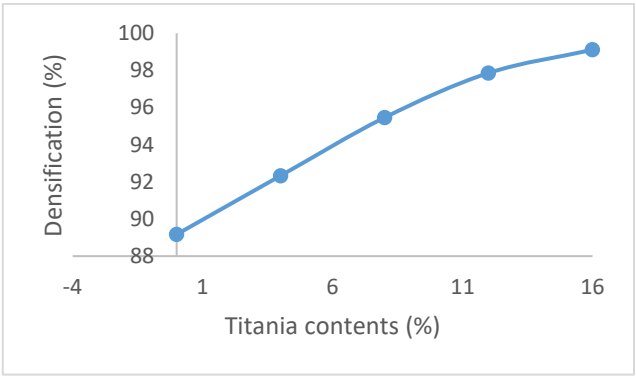

Figure 3. Effect of titania contents on the densification of the samples

3.2.2. Porosity

Figure 4 shows the effect of titania contents on the porosity of the samples. From the figure, it is observed that the porosity of the samples decreases with increase in the titania contents. It is observed the porosity of the sample with 0% titania (sample A) was at its highest of 10.83%, this is observed to decreased to 7.67% when the titania content was increased to 4% (sample B). The porosity is seen to further decrease to about 4.54% when the titania content was increased to 8% (sample C). Moreover, when the titania content was increased to 12% (sample D) the porosity is observed to reduce to 2.14%. At 16% titania content (sample E) the porosity of the sample is observed to reduce to its lowest of 0.89%. This is in agreement with the observation of other researchers (Aramide et al. 2017; Aramide, 2012). This is expected because densification means the elimination of pores from the sample (Brasileiro *et al.* 2006).

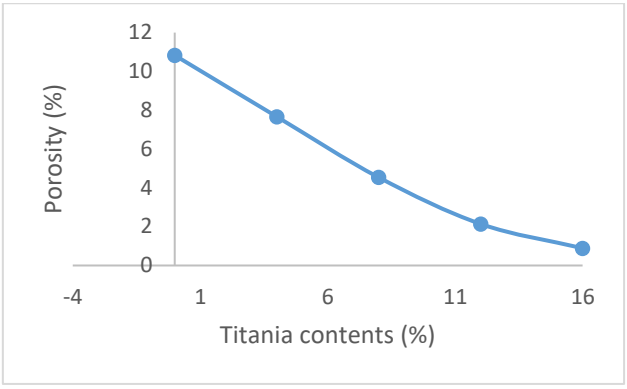

Figure 4. Effect of titania contents on the porosity of the samples

3.2.3. Hardness

The effect of titania content on the hardness of the samples is depicted in Figure 5. From the figure it is observed that the hardness of the samples increases with increased titania content. It is observed that the hardness of the sample was 455 Hv when its titania content was 0%, it increased to 499 Hv when its titania content was increased to 4%. Moreover, its hardness was raised to 564 Hv when it has a titania content of 8%, it further increased to 644 Hv with increase in its titania content to 12%. The hardness of the sample further increase to 817 Hv when its titania content was increased to 16%. The progressive increase in the hardness of the samples cannot be unconnected with the phases developed in the samples during sintering.

It is observed from Figure 1 that in sample A (0% titania), the identified phases are silimanite, cristobalite, graphite and pyroxmangite this is why it has the lowest hardness. For sample B (4% titania), the phases identified in it are silimanite, graphite, Mn_2O_7, quartz, Al_2TiO_4 and Mn_5Si_2, the development of Mn_2O_7, Al_2TiO_4 and Mn_5Si_2 phases in the sample could account for the increase in the hardness. Furthermore for sample C (8% titania) the identified phases are silimanite, carbon 60 (C60), Mn_2TiO_4, spessartine ($Mn_3Al_2Si_3O_{12}$), ramsdellite (MnO_2), graphite, alumina, rutile, stishovite (a form of silica), pyroxmangite. The evolvement of carbon 60 (C60), Mn_2TiO_4, spessartine ($Mn_3Al_2Si_3O_{12}$) and alumina could be said to influence the further increase in the hardness of the sample. Moreover, for sample D (12% titania) the phases identified in it are silimanite, graphite, cristobalite, ramsdellite, alumina, Ti_8O_{15} and mullite.

The existence of mullite and Ti_8O_{15} within ceramic matrix could be said to further improve on the hardness of the sample. Lastly, for sample E (16% titania) the identified phases are kyanite (an allotrope of silimanite), spessartine, alumina, rutile, Mn_2O_3, quartz, Al_4C_3 and $Al_4Si_2C_5$. It could be said that the development of carbides within the ceramic matrix is responsible for the increased hardness of the sample.

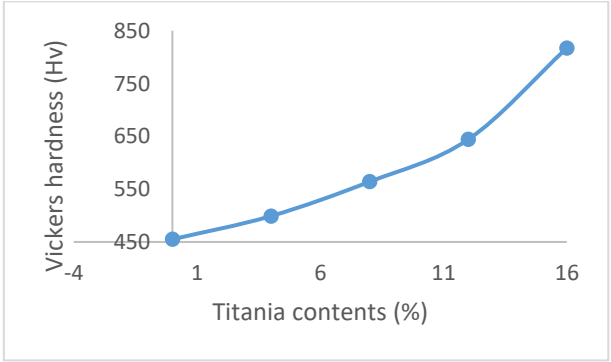

Figure 5. Effect of titania contents on the hardness of the samples

4. CONCLUSION

It is concluded that; the presence of Mn2O3 in the sample lead to formation of silimanite in preference to mullite when sintered above 900°C; 12% titania in the sample aided the formation of mullite phases within the sample; presence of 16% titania and Mn2O3 led to the formation of carbides like Al4C3 and Al4Si2C5 in the sample; addition of titania to the samples progressively improved on the densification of the sample with increased titania contents; development of carbides within the ceramic matrix is responsible for the increased hardness of the sample.

ACKNOWLEDGEMENT

The financial assistance of The World Academy of Science (TWAS) in collaboration with National Research Foundation (NRF) towards this research is hereby acknowledged. Opinions expressed and conclusions arrived at, are those of the authors and are not necessarily to be attributed to TWAS and NRF.

REFERENCES

Aksay, I., Dabbs, D.M., Sarikaya, M., (1991): "Mullite for structural, electronic and optical applications". *J. Am. Ceram. Soc.* Vol. 74, pp. 2343-2358.

Aramide, F.O., Akintunde, I.B., Popoola, P.A., (2017), "Effects of titania and sintering temperature on the phase development and properties of sintered mullite-carbon composite synthesized from okpella kaolin", *ACTA TECHNICA CORVINIENSIS – Bulletin of Engineering* vol. 10, no. 4, pp. 121-130.

Aramide, F.O., (2012): "Production and Characterization of Porous Insulating Fired Bricks from Ifon Clay with Varied Sawdust Admixture", *Journal of Minerals and Materials Characterization and Engineering*, vol. 11, pp. 970-975.

Aramide, F. O., Alaneme, K. K., Olubambi, P. A. Borode, J. O., (2015): "In-Situ Synthesis of Mullite Fibers Reinforced Zircon-Zirconia Refractory Ceramic Composite from Clay Based Materials", *International Journal of Materials and Chemistry*, vol. 5, no. 6, pp. 127-139.

Aramide, F.O., (2012): "Effect of Firing Temperature on Mechanical Properties of Fired Masonry Bricks Produced from Ipetumodu Clay", *Leonardo Journal of Sciences*, vol. 11, no. 21, pp. 70-82.

Aramide, F.O., Popoola, P.A., (2017): "Effects of Titania-Silicon Carbide Additives on the Phase Development and Properties of Sintered Mullite-Carbon Composite", *Preprint*, doi:10.20944/preprints201709.0008.v1

Brasileiro, M.I., Oliveira, D.H.S., Lira, H.L., Santana, L.N.L., Neves, G. A., Novaes, A.P., Sasak, J.M. (2006): "Mullite Preparation from Kaolin Residue". *Material Science Forum*, 530-531, 625-630, 121.

Callister, W.D., (2007): "Materials science and engineering: an introduction", 7th ed. *John Wiley & Sons Inc.*

Dag, L. and Annette, M., (2007): "Advanced Materials and Structures and their Fabrication Processes", *Narvik University College, HiN*, pp. 55, 61

Gong, L., Kyriakides, S., Jang, W.Y., (2005): "Compressive response of open-cell foams. Part I: Morphology and elastic properties". *Int J Solid Struct*, vol. 42, pp. 1355–1379.

Guo, A.R., Liu, J.C., Wang, Y., Xu, H., (2012): "Preparation of porous lamellar mullite ceramics with whisker skeletons by electrospinning and pressure molding". *Mater Lett.* Vol. 74, pp. 107–110.

Jang, W.Y., Kraynik, A.M., Kyriakides, S., (2008): "On the microstructure of open-cell foams and its effect on elastic properties". *Int J Solid Struct*, vol. 45, pp. 1845–1875.

Kanaun, S., Tkachenko, O., (2008): "Effective conductive properties of open-cell foams". *Int J Eng Sci*, vol 46, pp. 551–571.

Kaya, C., Gu, X., Al-Dawery, I., Butler, E.G., (2002): "Microstructural development of woven mullite fibre-reinforced mullite ceramic matrix composites by infiltration processing", *Science and Technology of Advanced Materials*, vol. 3. No.1, pp. 35-44.

Kaya, C., Butler, E.G,, Selcuk, A., Boccaccini, A.R., Lewis, M.H., (2002): "Mullite (Nextel™ 720) fiber-reinforced mullite matrix composites exhibiting favorable thermomechanical properties". *J Eur Ceram Soc*, vol. 22, pp. 2333–4232.

Lamberov, A.A., Sitnikova, E.Yu. and Abdulganeeva, A.Sh., (2012): "Kinetic Features of Phase Transformation of Kaolinite into Metakaolinite for Kaolin Clays from Different Deposits", Russian Journal of Applied Chemistry, Vol. 85, No. 6, pp. 892–897

Li, B., Zhu, J.X., Jiang, Y., Lin, L., Liu, Y., Chen, Z.F., (2012a): "Processing and flexural properties of 3D, seven-directional braided $(SiO_2)_f/SiO_2$ composites prepared by silica sol-infiltration-sintering method", *Ceram Int*, vol. 38, pp. 2209–2212.

Li, C., Chen, Z.F., Zhu, J.X., Liu, Y., Jiang, Y., Guan, T., et al. (2012b): "Mechanical properties and microstructure of 3D orthogonal quartz fiber reinforced silica compostite fabricated by silicasol-infiltration-sintering". *Mater Des*, vol. 36, pp. 289–295.

Low, I.M., Skala, R.D., Perera, D.S., (1994): "Fracture properties of layered mullite/zirconia-toughened alumina composites", *J. of Mater. Sc. Lett.*, vol. 13, pp. 1334-1336.

Moya, J. S. and Osendi M.I., (1983) "Effect of ZrO_2 (SS) in Mullite on the Sintering and Mechanical Properties of Mullite/ZrO_2 Composites," *Mater. Sci. Lett.*, vol. 2, pp. 599–601.

Naskar, M.K., Chatterjee, M., Dey. A., Basu, K., (2004): "Effects of processing parameters on the fabrication of near-net-shape fiber reinforced oxide ceramic matrix composites via sol–gel route". *Ceram Int.*, vol. **30**, pp. 257–65.

Osendi, M.I. and Baudin, C., (1996): "Mechanical Properties of Mullite Materials," *J. Euro. Ceram. Soc.*, vol. 96, pp. 217-224.

Sacks, M.D., Lee, H-W., Pask, J.A., (1990): "A review of powder preparation methods and densification procedures for fabricating high-density mullite", in: S. Somiya, R.F. Davies, J.A. Pask (Eds.) Ceramic Transactions, Mullite and Mullite Matrix Composites, Vol. 6, *American Ceramic Society*, Westerville, OH, pp. 167-207.

Stoll, E., Mahr, P., Kruger, H.G., Kern, H., Thomas, B.J.C., Boccaccini, A.R., (2006): "Fabrication technologies for oxide–oxide ceramic matrix composites based on electrophoretic deposition". *J Eur Ceram* vol. 26, pp. 1567–1576.

Tressler, R., (1999): "Recent developments in fibers and interphases for high temperature ceramic matrix composites". *Compos., Part A* vol. **30**, pp. 429–37.

Varga, G., (2007): "The structure of kaolinite and metakaolinite", *Építőanyag* 59. évf. 1. Szám pp. 6-9

Yang, W.S., Fuso, L., Biamino, S., Vasquez, D., Bolivar, C.V., Fino, P., et al. (2012a): "Fabrication of short carbon fibre reinforced SiC multilayer composites by tape casting". *Ceram Int*, vol. 38, pp. 1011–1018.

Yang, W.S., Biamino, S., Padovano, E., Fuso, L., Pavese, M., Marchisio, S., et al. (2012b): "Microstructure and mechanical properties of short carbon fiber/SiC multilayer composites prepared by tape casting". *Compos Sci Technol*, vol. 72, pp, 675–680.

Ye, F., Liu, L.M., Huang, L.J., (2008): "Fabrication and mechanical properties of carbon short fiber reinforced barium aluminosilicate glass–ceramic matrix composites". *Compos Sci Technol*, vol. 68, pp. 1710–1717.